Mechanics and Mechanical Engineering
Vol. 22, No. 2 (2018) 425–435

Numerical Analysis of the Rotor of a 30 kW ORC Microturbine Considering Properties of Aerodynamic Gas Bearings

Łukasz Breńkacz
Grzegorz Żywica
Małgorzata Bogulicz
Institute of Fluid Flow Machinery
Polish Academy of Sciences
Department of Turbine Dynamics and Diagnostics
Gdansk, Poland
lbrenkacz@imp.gda.pl

Received (23 June 2018)
Revised (9 August 2018)
Accepted (23 August 2018)

The paper focuses on the analysis of a 30 kW microturbine operating in the organic Rankine cycle (ORC) with a low-boiling working medium. The nominal speed of the rotor is 40,000 rpm. The investigated microturbine is an oil-free machine, which means that its bearings use the ORC working medium as a lubricant. We created a numerical model, which was used to assess the dynamic properties of the newly designed microturbine. The conducted analyses covered, inter alia, the optimization of some geometrical parameters of each bearing in order to cause the lubricating film to be created at a correspondingly low rotational speed as well as to obtain optimal dynamic properties of the system. The article provides a full dynamic picture of the rotor supported by two aerodynamic gas bearings. The included graphs demonstrate the vibration amplitude of the shaft as a function of the rotational speed as well as the results of the modal analysis in the form of natural vibration modes of the system and their corresponding natural frequencies.

Keywords: microturbine, dynamic analysis, rotor dynamics, gas bearings, organic Rankine cycle.

1. Introduction

Power turbines are the subject of many analyzes, the aim of which may be not only to increase their power output and efficiency but also to improve dynamic properties. Żywica et al. [1] described an analysis of the dynamic performance of an ORC microturbine with an electric power of 3 kW. New bearing systems and existing constructions are under development. Sung et al. [2] presented the performance tests carried out on the ORC system equipped with a 200 kW turbine. They used this system in a steel processing plant. The paper also shows how to

cool bearings in order to prevent their damage. When designing a bearing system it is important to ensure stable operating conditions, which means minimizing the vibration level at the nominal speed and making sure that the system can operate properly in the widest possible range of rotational speeds.

Lecompte et al. [3] wrote that ORC systems have different configurations for different operating conditions and vapor microturbines installed in those systems operate at various operating parameters (e.g. rotational speed). Furthermore, their rotor disks are subjected to various loads. Lee et al. [4] discussed the impact of the partial admission of a supersonic impulse turbine on its efficiency and the vibration level. The authors analyzed the vibration of the supporting structure depending on the partial admission ratio. Żywica et al. [5] presented an analysis of the dynamic properties of an ORC microturbine during its run-up.

Bini and Colombo [6] described several interesting bearing systems for a large ORC microturbine, one of which was patented. A typical bearing system consists of two bearings with a generator situated between them and a rotor disk mounted at one end of the rotor. The authors investigated two arrangements of the bearings. The calculation results obtained from the analysis of the first arrangement showed that the rotor with several turbine disks installed on one of its ends had a high vibration level at the nominal rotational speed. In the second arrangement, the distance between the bearings and turbine disks was different than in the first arrangement and the rotor was capable of operating at a nominal rotational speed without any signs of resonance.

Foil bearings, still considered as non-conventional solutions, are potentially very good in supporting rotors in ORC microturbines. Static and dynamic analyzes conducted on foil bearings are presented in two papers. The first paper was written by Żywica et al. [7] and the second by Bonello and Hassan [8]. Tkacz et al. [9] described the numerical methods used for investigating the dynamic performance of such bearings. Żywica et al. [10] presented the dynamic properties of a rotor supported by foil bearings. Bagiński et al. [11] conducted the research on the impact of cooling a foil bearing on the dynamic performance of the rotating system in which it was installed.

In ORC systems, various types of expanders (including scroll expanders [12] and microturbines [13, 14]) are employed as expansion devices. The key subassembly of an ORC system is a turbogenerator that consists of an expansion device coupled with a generator. It allows converting thermal energy into electricity.

According to the adopted design concept of the turbogenerator, we will mount the rotor disk of the microturbine on the same shaft as the generator's rotor, thus creating a compact and durable construction. As far as the turbogenerator's rotor is concerned, the results of research carried out so far show that the use of gas bearings powered with the vapor of a low-boiling medium seems to be the best choice. Using this type of bearings allows the turbogenerator to be oil-free. As the matter of fact, a small amount of the working medium (usually corresponding to a value of several percents of the flow rate of the fresh vapor) is enough to power such bearings.

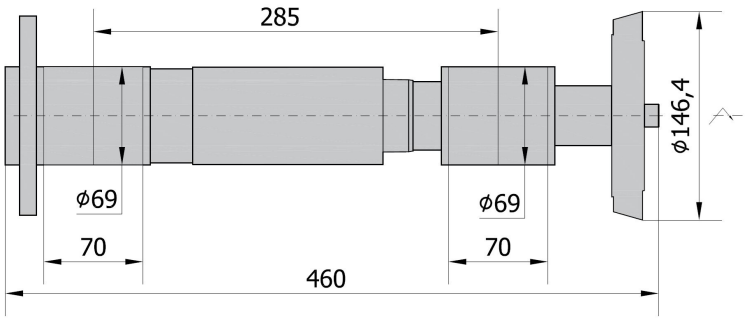

Figure 1 Basic dimensions of the rotor

In Fig. 1 we presented a scheme of the turbogenerator's rotor that was analyzed using FEM-based numerical simulations. The design concept includes the generator situated between a couple of radial gas bearings and a rotor disk (of the single-stage impulse turbine) placed on a free end of the shaft. Because the shaft has to be kept in a proper axial position, a single reversible thrust bearing will be installed, which is to operate as a gas bearing powered with the vapor of a low-boiling medium. We will place both the rotor and the generator inside a hermetically sealed casing. In the following sections of this article we will discuss findings of the analyzes aimed at selecting a proper geometry of the gas bearings as well as investigating the dynamic properties and strength of the ORC turbogenerator prototype.

2. Numerical computations of gas bearings

Within the framework of the research presented herein, we carried out an optimization of the geometry of the bearings by which the rotor of the designed turbogenerator is supported. Kiciński [15] described the results of calculations made using computer programs that belong to the MESWIR system. Tkacz et al. [16] described an isothermal model of gas bearings, which was also implemented in the MESWIR system. It was used to determine the characteristics of aerodynamic gas bearings. Both static and dynamic analysis was conducted. The static analysis consists in calculating a reaction force of the gaseous film to the static load resulting from the weight of the shaft. This force arises as a result of the rotational movement of the journal relative to the immovable sleeve owing to the viscosity of the lubricant. Calculations can be made for any gaseous medium, provided that its dynamic viscosity under given ambient conditions is known. The dynamic analysis consisted in the calculation of stiffness and damping coefficients for a fixed rotational speed, taking into account the static load that was calculated earlier.

Kinetostatic calculations were carried out using the KINWIR-G program (implemented into MESWIR system) into which were inserted the dynamic coefficients of gas bearings, calculated in the above-described manner. In this program, it is possible to model a series of complex structural subassemblies mutually coupled with each other. These subassemblies may include, among other things, a line of rotors with imperfections such as cracks, misalignments, slide bearings and the sup-

porting structure (bearing supports and foundation). From the mathematical point of view, the model considered herein can be described using the following non-linear differential Equations (1):

$$\mathbf{M}\ddot{\mathbf{x}} + \mathbf{D}\dot{\mathbf{x}} + \mathbf{K}\mathbf{x} = \mathbf{P}(t) \tag{1}$$

where:

$\mathbf{M}$ – global matrix of inertia,
$\mathbf{D}$ – global matrix of damping,
$\mathbf{K}$ – global matrix of stiffness,
$\mathbf{x}$, $\dot{\mathbf{x}}$, $\ddot{\mathbf{x}}$ – generalized vectors of displacements, velocities and acceleration,
$\mathbf{P}$ – generalized vector of external excitations
t – time.

Due to similar loads of two bearings of the projected system, we assumed that both of them would have the same geometry. Considering the overall dimensions of the generator, we decided that the bearings would have a diameter of 69 mm. This value is due to the fact that during placing the rotor inside the casing the generator rotor will have to pass through the sleeve of one of the bearings. Therefore, the internal diameters of the bearing sleeves must be larger than the external diameter of the generator rotor. On the other hand, the diameter of the bearing journals could not be greater than the internal diameter of the generator stator. Therefore, the diameter of bearings was predetermined and could not be optimized.

In order to select the bearings' length and radial clearance, we conducted a series of calculations. The smaller the lubrication gap, the lower the rotational speed at which the lubrication film was formed. The lubrication gap cannot be decreased too much because the bearings will not be possible to be manufactured due to technological reasons.

The wider the bearing, the lower the lift-off speed was. In this case, we also encounter some restrictions. Increasing the bearing length too much causes problems with its manufacture and accurate alignment of the sleeves. Bearing in mind the technological and structural limitations, we conducted a series of dynamic calculations that allowed us to choose optimal values for the length of the bearing and the size of its lubrication gap. A length of 70 mm and a radial clearance of 35 μm were considered the most appropriate and reliable geometrical parameters of the analyzed bearing. These are the parameter values that ensure the formation of a lubrication film at the lowest possible rotational speed, and at the same time will allow the whole system to be manufactured without any problems.

2.1. *Determination of stiffness and damping coefficients of the lubrication film*

In order to determine stiffness and damping coefficients of the lubrication film in the bearings in question, we developed a FEM model of the turbogenerator's rotor (see Fig. 2). The model comprises 24 Timoshenko-type beam elements, which had 4 degrees of freedom in each node for the purposes of kinetostatic numerical simulations. What is more, we incorporated four rigid disks into the model. The two of the disks have served to model the generator. The next two (on the right-hand side on the Fig. 2) modeled the rotor disk. The rotor has a length of 460 mm and

its total mass equals to 12.2 kg. Steel with a density of 7,860 kg/m^3 was selected as a material for the beam elements whilst disks had a density of 2,720 kg/m^3 — which corresponds to the density of aluminum. According to the findings of the above-mentioned analyzes, the geometrical parameters of both bearings are as follows: journal diameter – 69 mm, length – 70 mm, and radial clearance – 35 μm. The distance between the bearings is 285 mm.

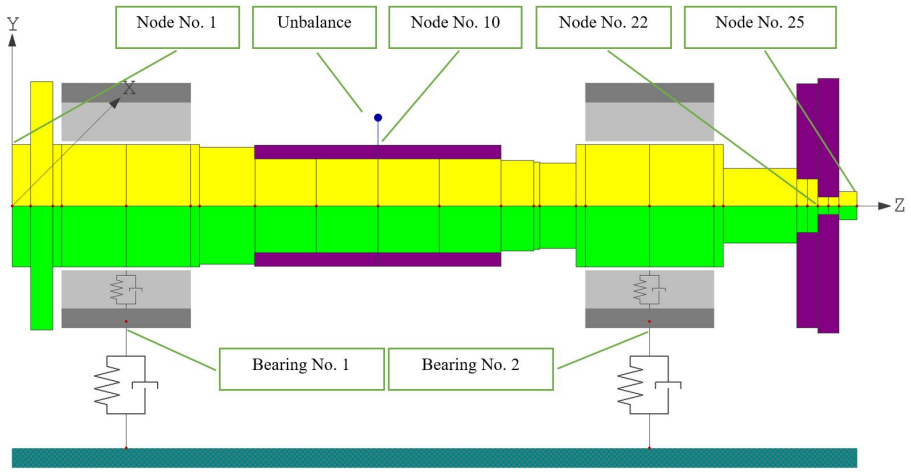

Figure 2 FEM model of the rotor

Within the framework of preliminary calculations, kinetostatic loads of the bearings were determined, which were approx. 61.1 N and 58.5 N respectively for the first and second bearing. When we knew the geometry and load of the bearings, we were able to determine stiffness and damping coefficients of the gaseous lubricating film. Their calculated values obtained at a speed of 40,000 rpm (the nominal speed) are in Table 1.

Table 1 Stiffness and damping coefficients of both bearings

Bearing No.	Coefficient	Denotation	Value	Unit
1	Stiffness	k_{xx}	0.211×10^8	N/m
1	Stiffness	k_{yy}	0.214×10^8	N/m
1	Damping	c_{xx}	0.792×10^4	Ns/m
1	Damping	c_{yy}	0.804×10^4	Ns/m
2	Stiffness	k_{xx}	0.211×10^8	N/m
2	Stiffness	k_{yy}	0.214×10^8	N/m
2	Damping	c_{xx}	0.791×10^4	Ns/m
2	Damping	c_{yy}	0.803×10^4	Ns/m

3. Modal analysis

Within the framework of the research described herein, we conducted a modal analysis of the rotor, namely, we determined eigenfrequencies and eigenmodes. The first ten natural frequencies of the rotor are in Table 2, with a short description of their corresponding eigenmodes.

Table 2 The first ten eigenfrequencies and eigenmodes of the rotor

No.	Frequency [Hz]	Eigenmode description
1	1.44	axial vibrations
2	48.01	torsional vibrations
3	259.24	lateral vibrations (conical mode)
4	277.16	lateral vibrations (cylindrical mode)
5	278.94	lateral vibrations (cylindrical mode)
6	289.43	lateral vibrations (conical mode)
7	939.97	bending vibrations
8	1099.79	bending vibrations (Fig. 3a)
9	1681.85	torsional vibrations
10	2416.27	bending vibrations (Fig. 3b)

The seventh and eighth eigenmode are the first two bending vibration modes, and the speeds at which they occurred are 56,398 rpm and 65,987 rpm, respectively. The shape of the eighth eigenmode is shown in Fig. 3a. As far as the dynamics of the analyzed rotor is concerned, bending vibration modes occurring at speeds that are close to the nominal speed should be given a lot of attention to prevent a resonance. The tenth eigenmode occurs at a rotational speed of 144,976 rpm. It is the second bending vibration mode shape of this system, which is characterized by three nodes (two side nodes and one middle node) and two antinodes situated between the middle node and the side nodes (Fig. 3b).

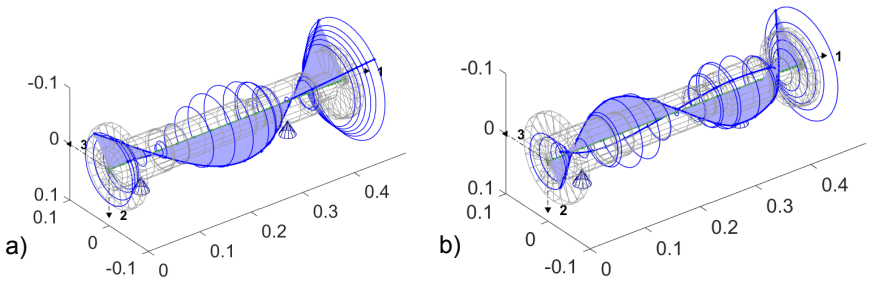

Figure 3 a) The eighth eigenmode of the rotor occurring at a speed of 65,987.1 rpm. b) The tenth eigenmode of the rotor occurring at a speed of 144,976.5 rpm.

The first and second bending vibration modes can be very dangerous from the point of view of the dynamics of the system. As the matter of fact, the speed at which the second bending vibration mode shape occurs is over three times higher than the nominal speed of the rotor.

Most importantly, none of the critical mode shapes will occur during the operation of the turbine at its nominal speed (40,000 rpm). The rotor is subcritical, which means that its nominal rotational speed is less than the first bending resonance speed.

4. Forced vibration analysis

Within the framework of the research described herein, we carried out a harmonic response analysis. For the calculation purposes, the unbalance equal to 7.32 gmm was selected based on the ISO 1940-1 standard [17]. The unbalance was located between the bearings. As a result of the carried out analysis, we obtained a graph demonstrating the vibration amplitude as a function of the rotational speed (Fig. 4). When we look at the curves, it is clear that the resonant speed is 70,000 rpm. The resonant speed is marked with a vertical blue line whilst the grey area shows the speed range in which the lowest and highest speeds are respectively 20 percent lower or higher than the nominal speed. The conducted analysis indicates that the operation of the rotor at each and every speed included in the speed range marked with the grey area is stable. The increase in the vibration level at speeds close to a speed of 70,000 rpm is connected with the first bending vibration mode shape. The stiffness and damping coefficients of the bearings did not have a big influence on this increase. Furthermore, the bearings are situated at the vibration nodes.

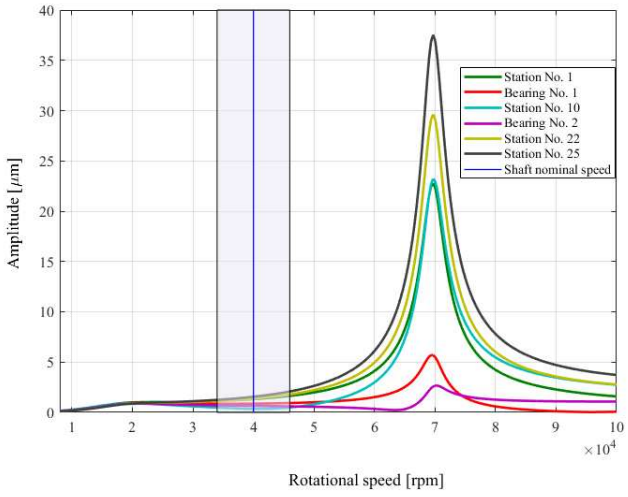

Figure 4 Amplitude vs. rotational speed curves obtained during the forced vibration analysis of the rotor of a 30 kW microturbine

5. Campbell diagram

Within the framework of the research described herein, a Campbell diagram was plotted (Fig. 5). It shows the computed eigenfrequencies as a function of the shaft's rotational speed. On the plot are three red skew lines representing respectively the first, second, and third harmonic speed of the rotor. The nominal speed is marked with a blue vertical line whilst the grey area around it indicates the speed range in which the lowest and highest speeds are respectively 15 percent lower or higher than the nominal speed. The most important, from the point of view of the dynamics of the system, is the fact that inside the grey area the three red skew lines do not intersect with the lines representing the natural frequencies. This result means that if the rotor would rotate at its nominal speed no eigenmodes would occur.

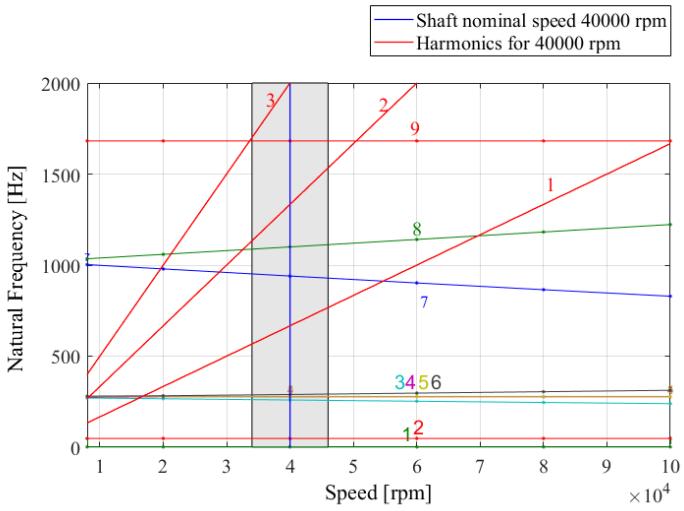

Figure 5 Campbell diagram of the rotor of a 30 kW microturbine

We conducted also the strength analysis of the rotor with turbine wheel using the finite element method (FEM). We took into account the full geometry of the rotor disk, including the three-dimensional geometry of the blades. The highest stress is 182.5 MPa and occurs near the middle hole and the hole for mounting a pin. The farther away from the center of the disk, the stresses are smaller and rarely exceed a value of 100 MPa. The stress magnitudes are also small near the blades. The stresses do not exceed a value of 70 MPa at the blade roots and decrease towards the tips. The analysis of the stress and displacement distributions showed that, as expected, the highest displacements occurred at the blade tips, i.e. they reached 68.5 μm. As the displacements of the blade tips do not exceed a value of 70 μm they are at an acceptable level.

6. Summary and conclusions

The article presents the results of analyzes related to the design of the rotor of a 30 kW turbine generator as well as to the selection of its bearing system. Within the framework of the research, we analyzed the rotor supported by aerodynamic bearings. Based on the CAD model, we created a numerical model, which we used to perform calculations using the finite element method. The numerical model of the rotor used for the dynamic analysis consists of beam elements (including appropriately modeled disks). The rotor was supported by two bearings whose geometrical parameters were optimized.

In the first part of numerical calculations, the focus was on determining the geometry of bearings as well as their stiffness and damping coefficients. In order to estimate the length and radial clearance of the bearings a series of calculations were made and the minimum rotational speeds at which a lubricating film forms itself (depending on the load) were obtained. The formation of a lubricating film gives an indication of the stable operation of an aerodynamic bearing. Having conducted a number of analyzes, we can say that the most appropriate magnitude of the radial clearance is 35 μm. In order to determine stiffness and damping coefficients of the lubricating film in the bearings, we developed a FEM model of the turbine generator's rotor. On its basis, a kinetostatic load of the bearings was calculated, which was followed by an estimation of their stiffness and damping coefficients.

We used modal analysis to obtain first ten eigenmodes and their corresponding eigenfrequencies. None of the calculated eigenmodes can be excited by the rotor unbalance at the speeds close to the nominal speed. Results of the forced vibration analysis show that the resonant speed is about 70,000 rpm. As this speed is much higher than the nominal speed (40,000 rpm) it is of no importance in terms of the dynamics of the investigated rotating system. The plotted Campbell diagram is a proof that the designed system has good dynamic properties, which means that the operation of the rotor at a nominal frequency (or its harmonics) would not cause any of the eigenmodes to occur.

The results of the strength analysis conducted on the rotor disk show that both the values of the reduced stress and of displacements of the tips of the microturbine's blades are at an acceptable level. At the nominal speed, we noticed the maximum reduced stresses (reaching 182.5 MPa) near the hole located in the middle of the rotor disk and they were circumferential stress concentrations. The stress magnitudes were significantly smaller at the blade roots and did not exceed a value of 70 MPa. On the whole disk, the stress values were several times smaller than the yield point of the selected construction material. The maximum displacements within the entire surfaces of the blades did not exceed a value of 70 m, which are acceptable.

To sum up, the obtained results of analyzes are a proof that the rotor supported by gas bearings has good static and dynamic properties and the total effort of the disk construction is acceptable. This means that the proposed design concept of the rotor is correct and we can use it to develop the final version of this microturbine subassembly.

7. Acknowledgements

This work has been funded by the National Centre for Research and Development from the Smart Growth Operational Programme (European funds) within project No. POIR.01.01.01-00-0512/16 carried out jointly with the Marani Sp. z o.o. company.

References

[1] **Żywica, G., Drewczyński, M., Kiciński, J., Rządkowski, R.**: Computational modal and strength analysis of the steam microturbine with fluid-film bearings, *Journal of Vibrational Engineering and Technologies*, 2, 6, 543–549, **2014**.

[2] **Sung, T., Yun, E., Kim, H. D., Yoon, S. Y., Choi, B. S., Kim, K., Kim, K. C.**: Performance characteristics of a 200-kW organic Rankine cycle system in a steel processing plant, *Applied Energy*, 183, 623–635, **2016**.

[3] **Lecompte, S., Huisseune, H., Van Den Broek, M., Vanslambrouck, B., De Paepe, M.**: Review of organic Rankine cycle (ORC) architectures for waste heat recovery, *Renewable and Sustainable Energy Reviews*, 47, 448–461, **2015**.

[4] **Lee, H. G., Shin, J. H., Choi, C. H., Jeong, E., Kwon, S.**: Partial admission effect on the performance and vibration of a supersonic impulse turbine, *Acta Astronautica*, 145, 105–115, **2018**.

[5] **Żywica, G., Kaczmarczyk, T. Z., Ihnatowicz, E., Turzyński, T.**: Experimental investigation of the domestic CHP ORC system in transient operating conditions, *Energy Procedia*, 129, 637–643, **2017**.

[6] **Bini, R., Colombo, D.**: Large multistage axial turbines, *Energy Procedia*, 129, 1078–1084, **2017**.

[7] **Żywica, G., Kiciński, J., Bagiński, P.**: The static and dynamic numerical analysis of the foil bearing structure, *Journal of Vibrational Engineering and Technologies*, 4, 3, 213–220, **2016**.

[8] **Bonello, P., Hassan, M. F. B.**: An experimental and theoretical analysis of a foil-air bearing rotor system, *Journal of Sound and Vibration*, 413, 395–420, **2018**.

[9] **Tkacz, E., Kozanecki, Z., Kozanecka, D.**: Numerical methods for theoretical analysis of foil bearing dynamics, *Mechanics Research Communications*, 82, 9–13, **2017**.

[10] **Żywica, G., Bagiński, P., Breńkacz, Ł., Miąskowski, W., Pietkiewicz, P., Nalepa, K.**: Dynamic state assessment of the high-speed rotor based on a structural-flow model of a foil bearing, *Diagnostyka*, 18, 1, 95–102, **2017**.

[11] **Bagiński, P., Żywica, G., Lubieniecki, M., Roemer, J.**: The effect of cooling the foil bearing on dynamics of the rotor-bearings system, *Journal of Vibroengineering*, 20, 2, 843–857, **2018**.

[12] **Song, P., Wei, M., Shi, L., Danish, S. N., Ma, C.**: A review of scroll expanders for organic Rankine cycle systems, *Applied Thermal Engineering*, 75, 54–64, **2015**.

[13] **Mounier, V., Olmedo, L. E., Schiffmann, J.**: Small scale radial inflow turbine performance and pre-design maps for Organic Rankine Cycles, *Energy*, 143, 1072–1084, **2018**.

[14] **Kaczmarczyk, T. Z., Żywica, G., Ihnatowicz, E.**: The impact of changes in the geometry of a radial microturbine stage on the efficiency of the micro CHP plant based on ORC, *Energy*, 137, 530–543, **2017**.

[15] **Kiciński, J.**: Dynamics of rotors and slide bearings (in Polish), *Gdańsk: IMP PAN, Maszyny Przepływowe*, **2005**.

[16] **Tkacz, E., Kozanecki, Z., Kozanecka, D., Łagodziński, J.**: A Self-Acting Gas Journal Bearing with a Flexibly Supported Foil — Numerical Model of Bearing Dynamics, *International Journal of Structural Stability and Dynamics*, 17, 5, 1740012, **2017**.

[17] ISO 1940-1 Mechanical vibration - balance quality requirements for rotors in a constant (rigid) state. Part 1: Specification and verification of balance tolerances, **2003**.